# Global Optimization for Sustainable Design and Synthesis of Algae Processing Network for $CO_2$ Mitigation and Biofuel Production Using Life Cycle Optimization

**Jian Gong and Fengqi You**
Dept. of Chemical and Biological Engineering, Northwestern University, Evanston, IL 60208

*DOI 10.1002/aic.14504*
*Published online June 9, 2014 in Wiley Online Library (wileyonlinelibrary.com)*

*Global optimization for sustainable design and synthesis of a large-scale algae processing network under economic and environmental criteria is addressed. An algae processing network superstructure including 7800 processing routes is proposed. Based on the superstructure, a multiobjective mixed-integer nonlinear programming (MINLP) model is developed to simultaneously optimize the unit cost and the unit global warming potential (GWP). To efficiently solve the nonconvex MINLP model with separable concave terms and mixed-integer fractional terms in the objective functions, a global optimization strategy that integrates a branch-and-refine algorithm based on successive piecewise linear approximations is proposed and an exact parametric algorithm based on Newton's method. Two Pareto-optimal curves are obtained for biofuel production and biological carbon sequestration, respectively. The unit annual biofuel production cost ranges from \$7.02/gasoline gallon equivalent (GGE) to \$9.71/GGE, corresponding to unit GWP's of 26.491 to 16.52 kg $CO_2$-eq/GGE, respectively.*  *AIChE J*, 60: 3195–3210, 2014
*Keywords: algal biodiesel, superstructure optimization, life cycle assessment, technoeconomic analysis, mixed-integer fractional programming*

## Introduction

Renewable biofuel is considered a promising fossil fuel substitute due to its potential for large-scale production and carbon mitigation.[1] Among various biomass feedstocks with increasing attention in the recent decades, algal biomass offers significant advantages over conventional energy crops. Algae have a high area productivity and accumulate lipid materials up to 80% of its dry cell weight.[2] They are able to utilize nonarable land and waste water for cultivation. Additionally, the hydrocarbon algal biofuels converted via hydroprocessing (Hyd.) accommodate the specifications of drop-in fuels, which can be directly incorporated into the existing infrastructure.[3]

To reduce environmental impacts and improve the overall economic performance, systematic modeling and optimization frameworks can be used to identify and assess the sustainable design and synthesis of a processing network.[4–6] Therefore, applying such a framework to the algae processing network provides valuable insights into the technology pathways in the context of sustainability. This in turn allows for a better understanding of the technology development. The goal of this research is to identify and assess the optimal sustainable design and synthesis of an algae processing network with both economic and environmental concerns.

In this work, we propose a superstructure of an algae processing network that integrates several algae cultivation technologies with a variety of downstream processing technologies. The superstructure is further improved by considering water and nutrients recycling, limiting algae growth to the day, and incorporating hydrothermal liquefaction (HTL) and utility generation. As a result, the proposed superstructure consists of 7800 processing routes in total and 11 processing sections, namely cultivation, harvesting, primary dewatering, secondary dewatering, storage, cell disruption and HTL, lipid extraction, upgrading, remnant treatment, electricity generation, and steam generation. Based on this superstructure, a new bicriteria mixed-integer nonlinear programming (MINLP) model for the sustainable design and synthesis is developed to simultaneously minimize the unit annualized cost and the unit global warming potential (GWP). As the final biofuel product can be biodiesel or renewable diesel depending on the specific upgrading technology, the unit objective functions are associated with the unit gasoline gallon equivalent (GGE) of the specific biofuel produced. To efficiently solve the problem, we propose a global optimization strategy that integrates a branch-and-refine algorithm based on successive piecewise linear approximations and an exact parametric algorithm based on Newton's method. The multiobjective optimization problem is solved with the $\varepsilon$-constraint method and results in two Pareto-optimal curves for biofuel production and biological carbon sequestration, respectively.

Additional Supporting Information may be found in the online version of this article.

Correspondence concerning this article should be addressed to F. You at you@northwestern.edu.

The main challenge of this work is to globally optimize the nonconvex MINLP model with separable concave terms and mixed-integer fractional terms in the objective functions. To the best of our knowledge, this class of MINLP problem has rarely been proposed before for large-scale superstructure optimization problems, as it could be computationally intractable due to its combinatorial nature and nonconvexity of objective functions.[4]

The novelties of this work are summarized below:

- A superstructure of an algae processing network including 7800 processing routes.
- A bicriteria nonconvex MINLP model for the sustainable design and synthesis of the algae processing network with separable concave terms and mixed-integer fractional terms in the objective functions.
- A global optimization strategy that integrates a branch-and-refine algorithm and a parametric algorithm.

The rest of this article is organized as follows. In the next section, we review existing literature closely related to this work and present the research needs and challenges. In the Problem Statement section, we describe the proposed algae processing network and provide necessary information of the optimization problem. The Model Formulation is given next with four types of constraints and two objective functions. In the Solution Approaches section, we present a global optimization strategy to enhance the computational performance. We discuss the resulting Pareto-optimal curves and the computational performance in the Results and Discussion section, followed by the conclusion at the end of the article.

## Literature Review

General information about algal biological properties and process technologies can be found in several reviews.[7–13] The technoeconomic analysis of algal biorefinery processes has been extensively studied. The opportunities of establishing algae-to-biofuel processes was evaluated for the British Columbia area.[14] Davis et al.[15] investigated the economics of autotrophic algae cultivation and conversion, resulting in production costs of $8.52/gal for open ponds and $18.10/gal for photobioreactors (PBRs). Following these results, they also reported a plausible production scenario after harmonizing several conclusions.[16] Delrue et al.[17] developed an model for process evaluation based on energetic, economic, and environmental criteria and concluded that a wet-lipid-extraction route performed better, but this route still had an unfavorable production cost. The same authors subsequently evaluated HTL, oil secretion, and alkane secretion in the algal processes.[18] Several simulation-based economic analyses indicated the bottlenecks for large-scale biodiesel production from algal biomass were cultivation and extraction operations.[19–21]

Many studies have performed life cycle analyses (LCA) for algal biorefinery processes. Lardon et al.[22] undertook a comparative LCA of biodiesel production from microalgae and concluded the best combination to be nitrogen starvation during cultivation followed by wet extraction. An LCA was presented by Brentner et al.[23] to compare more technologies in each step of the algal process for biodiesel production. Frank et al.[24,25] compared the LCA's of algal renewable diesel production with HTL and lipid extraction pathways. Another LCA study for algal biogas production and direct combustion also showed significant advantages in terms of energy recovery.[26]

Some works were focused on the superstructure optimization of bioenergy systems. Martin and Grossmann[27] recently studied the optimal algal composition for simultaneous production of bioethanol and biodiesel, resulting in 60% oil, 30% starch, and 10% protein. Baliban et al.[28] proposed an MINLP model to minimize the cost of a thermochemical conversion process from duckweed biomass to multiple energy products and applied a deterministic branch-and-bound global optimization strategy to solve the problem. The optimal design and operation of flexible polygeneration systems to coproduce power, liquid fuels, and chemicals from coal and biomass has been addressed with a two-stage formulation by Chen et al.[29] The same authors also proposed a decomposition method to efficiently optimize the corresponding problem.[30] The optimal design of another polygeneration system under both economic and environmental criteria demonstrated the potential for high energy efficiency and low emissions.[31] El-Halwagi et al.[32] recently introduced a new approach to incorporate safety criteria into the biorefinery optimization framework. Superstructure optimization of an eco-industrial park for heat integration resulted in significant savings.[33] A generic modeling approach for energy systems has been introduced to various superstructure optimization problems.[34–37] Similar superstructure optimization approaches have been applied for large-scale algal biofuel production from flue gas.[6,38]

Despite several contributions focusing on algal processes,[6,34,38] no algae processing network that integrates comprehensive algae processing technologies from gaseous carbon source to various biofuel products, considers water and nutrients recycling, and utility generation, limits algae growth to the day, and includes the most recent technologies such as HTL has been developed. The network proposed in this work addresses these research gaps and consists of 7800 processing routes in total. Furthermore, globally optimizing the corresponding nonconvex MINLP model including separable concave terms and mixed-integer fractional terms in the objective functions is the major challenge of this work, as the combinatorial and nonconvex nature could cause solving such problems computationally intractable with general-purpose solvers such as BARON 12.3.[39] In this study, we address this challenge with a novel global optimization strategy and efficiently obtain global optimal solutions.

## Problem Statement

### *Process description*

The proposed algae processing network starts with a gaseous carbon source, composed of 71.16% nitrogen, 21.14% carbon dioxide, 4.29% oxygen, and 3.41% water by weight.[40] Feed gas, off-gas, makeup nutrients, and recycled materials are simultaneously fed into the cultivation system. Microalgae *Chlorella vulgaris* with a C:N:P stoichiometric composition of 103:10:1 are cultivated in this system.[24] As much as 80% of the carbon dioxide is absorbed by algae and the unused gas is directly emitted to the atmosphere.[24] Following algae cultivation, mature algae slurry is concentrated by several technologies before utilization. First, 10% of the dilute slurry is harvested by auto flocculation and dissolved air flotation. The water content is further reduced by primary and secondary dewatering. Most of the reduced water, flocculants, and some of the algal cells are recycled to the cultivation facility. As light is an essential condition for

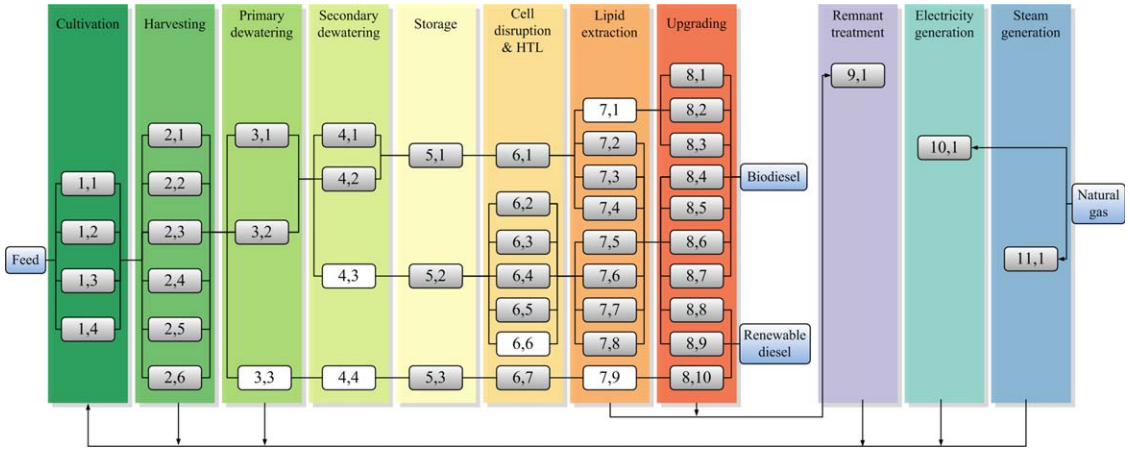


**Figure 1. Superstructure of an algae processing network.**

**<1,1> open pond;[41] <1,2> flat plate PBR;[41] <1,3> bubble column PBR;[41] <1,4> tubular PBR;[41] <2,1> flocculation with poly-electrolyte;[34] <2,2> flocculation with sodium hydroxide;[34] <2,3> flocculation with poly-aluminum chloride;[34] <2,4> flocculation with aluminum sulfate;[34] <2,5> flocculation with chitosan;[34] <2,6> flocculation with poly-γ-glutamic acid;[34] <3,1> centrifugation;[42] <3,2> pressure filtration;[13] <3,3> blank; <4,1> freeze drying;[10] <4,2> thermal drying;[6] <4,3> and <4,4> blank; <5,1>, <5,2>, and <5,3> biomass storage;[41] <6,1> bead beating;[43] <6,2> high pressure homogenization;[43] <6,3> bead beating;[43] <6,4> microwaving;[43] <6,5> sonication;[43] <6,6> blank; <6,7> HTL;[18,44] <7,1> blank; <7,2> hexane extraction;[45] <7,3> isopropanol/hexane extraction;[45] <7,4> supercritical $CO_2$ extraction;[45] <7,5> hexane extraction;[45] <7,6> isopropanol/hexane extraction;[45] <7,7> butanol extraction;[46] <7,8> supercritical $CO_2$ extraction;[45] <7,9> blank; <8,1> alkaline *in situ* transesterification;[34] <8,2> acidic *in situ* transesterification;[34] <8,3> enzymatic *in situ* transesterification;[34] <8,4> sodium-methoxide-catalyzed transesterification;[6] <8,5> supercritical methanol transesterification;[6] <8,6> enzyme-catalyzed transesterification;[6] <8,7> heterogeneous-catalyzed transesterification;[6] <8,8> Co/Mo-catalyzed hydroprocessing;[41] <8,9> Ni/Mo-catalyzed hydroprocessing;[41] <8,10> HZSM-5-catalyzed hydroprocessing;[47] <9,1> anaerobic digestion;[15] <10,1> electricity generation;[48] <11,1> steam generation.[49][Color figure can be viewed in the online issue, which is available at wileyonlinelibrary.com.]**

photosynthesis, algal cultivation, and dewatering technologies operate only during the day.[38] To keep downstream facilities operating continuously, we introduce a storage tank to temporarily store part of the enriched algae biomass produced during daytime operation for the production at night.

Next, the enriched microalgae paste undergoes cell disruption and lipid extraction or HTL so that most of the lipid materials are separated from algal cells. The lipid materials are then upgraded to biodiesel or renewable diesel depending on the specific conversion technologies. The rest of the algal body or remnant is fed to an anaerobic digester and decomposed into biogas, aqueous nutrients, and unreacted solids. The integration of remnant treatment into the algae processing network largely improves the energy utilization and reduces the total cost. Additionally, we couple electricity and steam generation into the network to satisfy the onsite energy consumption and reuse the resulting off-gas. Note that the algal processing network does not export extra utilities to the external market. An alternative way of meeting the energy demand is to directly purchase electricity and steam from the external market. Correspondingly, this choice could lead to lower costs but higher indirect greenhouse gas (GHG) emissions.

The superstructure uses a wide spectrum of technology alternatives as shown in Figure 1. It includes 11 sections: cultivation, harvesting, primary dewatering, secondary dewatering, storage, cell disruption and HTL, lipid extraction, upgrading, remnant treatment, electricity generation, and steam generation. Four types of algal cultivation devices are considered in the cultivation section: open pond, flat plate PBR, bubble column PBR, and tubular PBR.[38] Open pond cultivation requires less energy consumption and capital cost; in contrast, PBRs exhibit higher productivity. Depending on the specific technology selected, algae concentration in the "out" flow of the cultivation section is a parameter taken from existing literature.[24] The amount of algal biomass produced during cultivation is calculated based on the algal composition and carbon dioxide utilization efficiency. All related parameters can be found in the Supporting Information file. Six types of alternative flocculants presented in the harvesting section are poly-electrolyte, sodium hydroxide, poly-aluminum chloride, aluminum sulfate, chitosan, and poly-γ-glutamic acid. They differ from each other by the percentage of algal biomass that proceeds to the next section. Primary dewatering is accomplished by either centrifugation or pressure filtration. Centrifugation provides an algal paste of 32 wt % and consumes a large quantity of energy; pressure filtration, however, saves energy in exchange for a lower product concentration of 27%. If dry algae extraction is selected, the algal paste will be either freeze-dried or thermally dried in the secondary dewatering section so that the water content is reduced to 15 wt %. However, both drying technology consumes massive energy. If wet algal paste is used directly in lipid extraction, secondary dewatering will be bypassed. Note that all the white blocks denoted as "blank" represent bypassing of the section.

HTL is an emerging technology, which uses wet algal paste and produces more lipid materials than solvent extraction technologies as it converts a portion of the protein and carbohydrates into lipids.[44] However, this technology operates under the supercritical condition of water, leading to both high capital cost and high energy consumption. If HTL is used to process wet algae, primary dewatering, secondary dewatering, and lipid extraction will be bypassed accordingly. After dewatering sections, we store part of the microalgae biomass in a storage tank to supply the continuous production during night time operations. We consider five cell disruption technologies to improve lipid yields in the next section. Bead beating is used for both dry and wet algal biomass, whereas high pressure homogenization,

microwaving, and sonication are used to destroy only the wet algal cells. All the above disruption technologies consume a large amount of energy. Following the same assumption by Chisti, we consider 25 wt % of the raw algal biomass is made up of "lipids" and the rest algal body are treated as "remnant."[7] The above cell disruption methods determine the maximum portion of the total lipids that could be separated by extraction technologies. Seven extraction candidates are designed for various upstream conditions in the lipid extraction section. They are hexane extraction, isopropanol/hexane extraction, and supercritical $CO_2$ extraction for both dry and wet microalgae, as well as butanol extraction specifically for wet microalgae. In general, hexane extraction is the most widely accepted extraction process in conceptual algal process designs.[6,15,17] However, experiments show very poor practical effect when using hexane as the extractant.[45] According to the basic chemical principle of "like dissolving like," polar lipid molecules should be extracted predominantly by polar solvents rather than neutral hexane. Therefore, butanol and isopropanol are also used as alternative extractants in the proposed superstructure. Supercritical carbon dioxide extraction presents the best extraction efficiency for both dry and wet algae at the expense of extremely high energy consumption. The 10 upgrading technologies considered in this work can be divided into two categories according to their products. Transesterification (Trans.) results in fatty acid methyl esters or biodiesel, whereas Hyd. results in saturated hydrocarbons or renewable diesel that is capable of replacing fossil fuels directly. Hyd. technologies demand extra hydrogen and higher energy input. Specifically, we incorporate alkaline in situ Trans., acidic in situ Trans., enzymatic in situ Trans., sodium-methoxide-catalyzed Trans., supercritical methanol Trans., enzyme-catalyzed Trans., heterogeneous-catalyzed Trans., Co/Mo-catalyzed Hyd., Ni/Mo-catalyzed Hyd., and HZSM-5-catalyzed Hyd. Algal remnants separated from lipid extraction and upgrading sections are used in anaerobic digestion. Electricity generation and steam generation are onsite utility facilities using natural gas as the feedstock.

### *Assumptions*

- Algae growth depends only on water, carbon dioxide, nitrogen, and phosphorus nutrients; the recycled effluent from anaerobic digestion can be directly used for algae cultivation; growth rates in various technologies are constants during a year.
- The production distributions of anaerobic digestion of remnant materials from different technologies are assumed to be identical.
- A linear relationship between mass flow rate and energy consumption is assumed.

### *Given*

The superstructure of an algae processing network that considers various technological alternatives for the production of algal biofuels is given. Properties of the feed gas are known. The complete species set is also given. The other parameters involved in the calculation are listed below.

- Operating time of each technology in a year.
- Area productivities of each bioreactor.
- Conversion of each reaction.
- Stoichiometric coefficient of each reaction.
- Concentrations of necessary materials in the inlet flows.
- Split fraction of each species to both the next "down" flow and the "emission" flow (see Figure 2).
- Weight fraction of feed gas and natural gas, total mass flow rate of the flue gas.
- Natural gas combustion efficiency, heat exchanger efficiency, and turbine efficiency.
- Physical properties of different species.
- Unit heat and power consumption of each technology.
- Base case costs, mass flow rates, sizing factors, and chemical engineering plant cost index of each technology.
- Market prices of raw materials, utilities, and products.
- Percentage of project investment cost into the total capital cost.
- Life span of the biorefinery.
- Interest rate.
- Damage factors of the direct emissions, power, and heat in the life cycle environmental impact analysis.

### *Determine*

The goal of this problem is to determine the optimal sustainable processing route of the algae processing network by simultaneously minimizing the unit annualized cost and the unit GWP both associated with the unit GGE of the final biofuel produced. The mathematical model considers mass balance constraints, energy balance constraints, technoeconomic evaluation constraints, and life cycle environmental impact analysis constraints. The major decision variables include:

- Technology selection.
- Mass flow rate of each species in each flow.
- Electricity and heat consumption of each technology and energy generation from onsite utility facilities.
- Overall capital cost, operation cost, and revenue required for economic evaluation.
- Gate-to-gate life cycle environmental impact measured by GWP to account for both direct and indirect GHG emissions.

## Model Formulation

$$\min\ unit\_cost = \frac{a + \sum_{i\in I, j\in J} B_{i,j}\left(m_{i,j}^{cc}\right)^{SF_{i,j}}}{gge}$$

$$\min\ unit\_gwp = \frac{gwp}{gge}$$

(P1) s.t. mass balance constraints (1)−(18)

energy balance constraints (19)−(24)

economic evaluation constraints (25)−(39)

life cycle environmental impact analysis constraints (40)−(44)

The superstructure optimization model is formulated as a multiobjective MINLP problem which simultaneously minimizes the unit annualized cost and the unit GWP, subject to four types of constraints: mass balance constraints, energy balance constraints, economic evaluation constraints, and life cycle environmental impact analysis constraints. The generic form of the MINLP problem is given in (P1).

All the mass balance constraints, energy balance constraints, life cycle environmental impact analysis constraints, and some of the economic evaluation constraints are

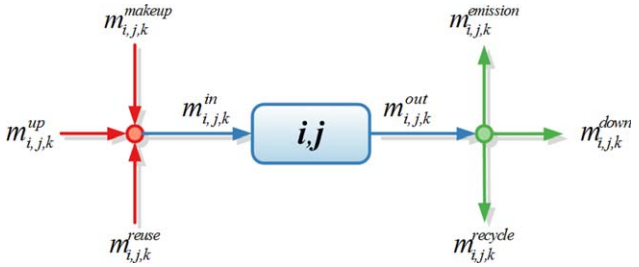


**Figure 2. Illustrative mass balance model of technology *j* in section of *i*.**

**[Color figure can be viewed in the online issue, which is available at wileyonlinelibrary.com.]**

formulated as linear equalities and inequalities. The nonlinear terms in the proposed model are separable concave functions for capital cost estimation and two fractional objective functions.

The index for the sections is denoted as $i$, whereas the index for alternative technologies is denoted as $j$. The elements and species occurring in the process superstructure are denoted as $k$. For clarity, we denote all the variables as lower case letters or letter combinations, whereas parameters are denoted as upper case letters and lower case Greek letters.

### *Mass balance constraints*

The mass balance constraints can be categorized into two groups. The first group describes the superstructure configuration with binary variables and logic constraints. The second group establishes a generic mass balance framework for each technology.

*Superstructure Configuration Constraints.* Equations 1–6 are formulated specifically to describe the configuration of the proposed superstructure. We introduce a binary variable $y_{i,j}$ to model the selection of technology $j$ in section $i$. If the technology is selected, $y_{i,j}$ equals 1; otherwise, $y_{i,j}$ equals 0. Equation 1 guarantees only one technology $j$ among the available alternatives is selected in section $i$. Equation 2 enforces that technologies <3,3>, <4,4>, <5,3>, <6,7>, <7,9>, and <8,10> are selected or bypassed simultaneously. Equation 3 requires that if either <4,1> or <4,2> is selected, technologies <5,1> and <6,1> have to be selected and technologies <7,5>, <7,6>, <7,7>, <7,8>, and <7,9> are bypassed from the lipid extraction section. In Eq. 4, if technology <7,1> is fixed in the cell disruption section, only <8,1>, <8,2>, and <8,3> are available in the upgrading section. Besides the above constraints, technologies <4,3> and <5,2> have to be selected simultaneously as described in Eq. 5.

$$\sum_{j\in J} y_{i,j}=1, \qquad \forall i \in I \tag{1}$$

$$y_{3,3}=y_{4,4}=y_{5,3}=y_{6,7}=y_{7,9}=y_{8,10} \tag{2}$$

$$y_{4,1}+y_{4,2}=y_{5,1}=y_{6,1}=y_{7,1}+y_{7,2}+y_{7,3}+y_{7,4} \tag{3}$$

$$y_{7,1}=y_{8,1}+y_{8,2}+y_{8,3} \tag{4}$$

$$y_{4,3}=y_{5,2} \tag{5}$$

$$0 \le m^{n}_{i,j,k} \le y_{i,j}\cdot UB^{m}, \qquad \forall i \in I, j \in J, k \in K, n \in N \tag{6}$$

Constraint 6 provides the lower and upper bounds of the mass flow rate $m^{n}_{i,j,k}$ of species $k$ in flow $n$ of technology $j$ in section $i$. In this constraint, $UB^{m}$ is the upper bound of the mass flow rate; superscript $n$ represents the flows involved in the generic mass balance framework. According to the harmonized study conducted by Davis et al.,[16] the upper bound of the mass flow rate is estimated to be $10^{8}$ t/h using the open pond cultivation system and Trans. process to produce biodiesel. Note that if a technology is bypassed, its binary variable will be 0 and the lower bounds and upper bounds will be 0 simultaneously, resulting in 0 for the corresponding mass flow rates.

*Generic Mass Balance Framework.* The generic mass balance framework proposed in this work uses three sequential steps in modeling each technology. These steps include an inlet converging step, a conversion step, and an outlet separation step. The involved flows and their relationships are illustrated in Figure 2. The inlet converging step, consisting of Eqs. 7–10, prepares the input flow by integrating an "up" flow, a "reuse" flow, and a "makeup" flow. Before the details of each constraint are given, we declare $i'$ and $k'$ the aliases for $i$ and $k$, respectively. Equation 7 defines the total mass flow rate of species $k$ in the "up" flow of section $i$ as the sum of corresponding "down" flows. $D_i$ is the subset of sections whose "down" flows go to section $i$. Likewise, Eq. 8 defines the "reuse" flow based on "recycle" flows, and $R_i$ is the subset of sections whose "recycle" flows go to section $i$. $P^{in}_{i,j,k,k'}$ is the concentration of species $k$ based on species $k'$ in the, "in" flow of technology $j$ in section $i$. Equation 10 defines the mass flow rate of the inlet flow $m^{in}_{i,j,k}$ by summing up the "up," "reuse," and "makeup" flows

$$\sum_{j\in J} m^{up}_{i,j,k}=\sum_{i'\in D_i, j\in J} m^{down}_{i',j,k}, \qquad \forall i \in I, k \in K \tag{7}$$

$$\sum_{j\in J} m^{reuse}_{i,j,k}=\sum_{i'\in R_i, j\in J} m^{recycle}_{i',j,k}, \qquad \forall i \in I, k \in K \tag{8}$$

$$m^{in}_{i,j,k}=\sum_{k'\in K}\left(P^{in}_{i,j,k,k'}\cdot m^{in}_{i,j,k'}\right), \qquad \forall i \in I, j \in J, k \in K \tag{9}$$

$$m^{in}_{i,j,k}=m^{up}_{i,j,k}+m^{reuse}_{i,j,k}+m^{makeup}_{i,j,k}, \qquad \forall i \in I, j \in J, k \in K \tag{10}$$

The conversion step includes only Eq. 11, which describes the chemical reaction occurring in the corresponding technology. $X_{i,j}$ is the reaction conversion of technology $j$ in section $i$; $SC_{i,j,k,k'}$ is the stoichiometric coefficient of species $k$ based on species $k'$ in the reaction of technology $j$ in section $i$.

$$m^{out}_{i,j,k}=m^{in}_{i,j,k}+\sum_{k'\in K}\left(SC_{i,j,k,k'}\cdot X_{i,j}\cdot m^{in}_{i,j,k'}\right), \qquad \forall i \in I, j \in J, k \in K \tag{11}$$

Finally, the outlet separation step from Eqs. 12–14 separates the reaction products into a "down" flow, a "recycle" flow, and an "emission" flow. As the separation equipment is included in the technology together with converging and conversion equipment, the split flows contains necessary fractions from the "out" flow. $SF^{down}_{i,j,k,k'}$ is the split fraction of species $k$ of technology $j$ in section $i$ to the "down" flow on the basis of species $k'$; $SF^{emission}_{i,j,k}$ is the split fraction of species $k$ of technology $j$ in section $i$ into the "emission" flow. As the "out" flow is defined as the sum of these three flows, the rest components remain in the corresponding "recycle" flow

$$m^{out}_{i,j,k}=m^{down}_{i,j,k}+m^{recycle}_{i,j,k}+m^{emission}_{i,j,k}, \qquad \forall i \in I, j \in J, k \in K \tag{12}$$

$$m_{i,j,k}^{down} = \sum_{k' \in K} \left( SF_{i,j,k,k'}^{down} \cdot m_{i,j,k'}^{out} \right), \qquad \forall i \in I, j \in J, k \in K \quad (13)$$

$$m_{i,j,k}^{emission} = SF_{i,j,k}^{emission} \cdot m_{i,j,k}^{out}, \qquad \forall i \in I, j \in J, k \in K \quad (14)$$

The entire superstructure has three initial flows, which are defined by Eqs. 15–17. $WF_k^{fg}$ and $WF_k^{ng}$ are the weight fractions of feed gas and purchased natural gas, respectively; $M^{fg}$ is the total mass flow of the feed flue gas; $m^{ng1}$ and $m^{ng2}$ are the total natural gas mass flow to the electricity and steam generation system, respectively

$$\sum_{j \in J} m_{1,j,k}^{up} = WF_k^{fg} \cdot M^{fg}, \qquad \forall k \in K \quad (15)$$

$$\sum_{j \in J} m_{10,j,k}^{up} = WF_k^{ng} \cdot m^{ng1}, \qquad \forall k \in K \quad (16)$$

$$\sum_{j \in J} m_{11,j,k}^{up} = WF_k^{ng} \cdot m^{ng2}, \qquad \forall k \in K \quad (17)$$

The algal processing network has two kinds of biofuel products, which are biodiesel from Trans. technologies and renewable diesel from Hyd. technologies. For the purpose of evaluating the unit economic and environmental performance of different processing routes, we calculate the total annual biofuel production on a GGE basis in Eq. 18, where $GGE_k$ is the volumetric conversion coefficient of species $k$, $H$ represents the annual operation time of the algae processing network, and $\rho^{diesel}$ is the density of diesel. In this work, the densities of biodiesel and renewable diesel are taken as the same

$$gge = \frac{H}{\rho^{diesel}} \cdot \sum_{j \in J, k \in K} \left( m_{8,j,k}^{down} \cdot GGE_k \right) \quad (18)$$

### Energy balance constraints

The energy balance of the proposed superstructure involves electricity and heat. In each category, we calculate the amount of energy consumption and generation based on the mass flow rates.

*Electricity.* The electricity consumption of section $i$ is modeled by Eq. 19 where $UPC_{i,j,k}$ is the unit power consumption of species $k$ of technology $j$ in the corresponding section

$$pc_i = \sum_{j \in J, k \in K} \left( UPC_{i,j,k} \cdot X_{i,j} \cdot m_{i,j,k}^{in} \right), \qquad \forall i \in I \quad (19)$$

The total electricity consumption of this algal processing network can be satisfied by directly purchasing electricity from the grid. An alternative way is to generate electricity onsite by combusting natural gas. The electricity generation rate is defined by Eq. 20, where $Y^{turbine}$ denotes the energy conversion efficiency of the turbine, $LHV_k$ represents the lower heating value of species $k$, and $G$ is the subset of species that are the major components in natural gas. As the onsite electricity generation system does not export power to the external market, constraint Eq. 21 requires the upper bound of the electricity produced to be the total power consumption.

$$pp = Y^{turbine} \cdot \sum_{k \in G} \left( LHV_k \cdot WF_k^{ng} \cdot m^{ng1} \right) \quad (20)$$

$$pp \le \sum_{i \in I} pc_i \quad (21)$$

*Heat.* The heat consumption and generation are defined by constraints 22–24 in a similar manner to electricity. $UHC_{i,j,k}$ is the unit heat consumption of species $k$ of technology $j$ in the corresponding section; $Y^{he}$ and $Y^{com}$ denote the energy conversion efficiency of the heat exchanger and combustor in the steam generation system, respectively.

$$hc_i = \sum_{j \in J, k \in K} \left( UHC_{i,j,k} \cdot X_{i,j} \cdot m_{i,j,k}^{in} \right), \qquad \forall i \in I \quad (22)$$

$$hp = Y^{he} \cdot Y^{com} \cdot \sum_{k \in G} \left( LHV_k \cdot WF_k^{ng} \cdot m^{ng2} \right) \quad (23)$$

$$hp \le \sum_{i \in I} hc_i \quad (24)$$

### Economic evaluation constraints

The goal of economic evaluation is to identify the unit annualized cost including both capital and operation costs.

$$cc_{i,j} = CC_{i,j}^b \left( \frac{m_{i,j}^{cc}}{MF_{i,j}^b} \right)^{SF_{i,j}} \left( \frac{CEPCI_{i,j}}{CEPCI_{i,j}^b} \right), \qquad \forall i \in I, j \in J \quad (25)$$

$$m_{i,j}^{cc} = \sum_{k \in C_i} m_{i,j,k}^{in}, \qquad \forall i \in I, j \in J \quad (26)$$

The capital cost of every technology is evaluated by a generic function in Eq. 25, where $CC_{i,j}^b$ is the capital cost of technology $j$ in section $i$ in the base case; $MF_{i,j}^b$ is the mass flow rate of technology $j$ in section $i$ in the base case; $SF_{i,j}$ is the sizing factor of technology $j$ in section $i$. We note that the sizing factor $SF_{i,j}$ ranges from 0 to 1, resulting in a number of concave terms. Furthermore, we use the chemical engineering plant cost index of the reference year $CEPCI_{i,j}$ and of the base year $CEPCI_{i,j}^b$ to account for inflation. The mass flow rate of $m_{i,j}^{cc}$ is defined by Eq. 26, where $C_i$ is the subset of species that contribute to $m_{i,j}^{cc}$ in section $i$.

$$land\_cost = PRICE^{land} \cdot \sum_{j \in J} \frac{m_{1,j,20}^{in}}{PRO_j^a} \quad (27)$$

The land cost, *land_cost*, of the algae processing network is evaluated by Eq. 27, where $PRICE^{land}$ is the unit land cost; $PRO_j^a$ is the area productivity of technology $j$ in the cultivation section

$$tpic = P^K \cdot \sum_{i \in I, j \in J} cc_{i,j} + land\_cost \quad (28)$$

The total project investment cost *tpic* is calculated by Eq. 28, and accounts for equipment capital costs, field materials and labor costs for installation, insurance, freight costs, construction costs, contractor engineering costs, and land costs.[50] $P^K$ is the total project investment cost multiplier based on the total capital cost. The annualized investment cost is calculated by Eq. 29, where $IR$ is the interest rate and $LS$ is the life span of this project in years[50]

$$aic = tpic \cdot \frac{IR \cdot (IR+1)^{LS}}{(IR+1)^{LS} - 1} \quad (29)$$

The annual operation cost aoc is quantified by Eqs. 30–34 as the sum of feedstock cost *fc*, utility cost *utility*, O&M cost *omc*, and waste disposal cost *waste*. In these equations, $PRICE_k$, $PRICE^{electricity}$, $PRICE^{steam}$, $PRICE^{ng}$, and $PRICE^{wd}$ are unit prices of related items or services; $P^{om}$ is the

percentage of the annualized investment cost into the O&M cost; $L$ is the subset of liquid species; $WR$ is the subset of sections whose "recycle" flow is discharged during nighttime productions; $T_{i,j}$ denotes the specific operating time of technology $j$ in section $i$. Note that since cultivation sections operate only during daytime, the "recycle" flow to the cultivation section is discharged during nighttime productions. As a result, parameter $NR$ is introduced to account for the ratio of night hours divided by the total hours in a day, and we assume the value of this parameter to be 0.5 in this study

$$aoc = fsc + utility + omc + waste \tag{30}$$

$$fsc = \sum_{i\in I, j\in J, k\in K} PRICE_k \cdot T_{i,j} \cdot m_{i,j,k}^{makeup} \tag{31}$$

$$utility = H \cdot \left[ PRICE^{\text{electricity}} \cdot \left( \sum_{i\in I} pc_i - pp \right) + PRICE^{steam} \cdot \left( \sum_{i\in I} hc_i - hp \right) + \frac{PRICE^{\text{ng}}}{\rho^{ng}} \cdot \left( m^{ng1} + m^{ng2} \right) \right] \tag{32}$$

$$omc = P^{om} \cdot aic \tag{33}$$

$$waste = PRICE^{wd} \cdot \left( \sum_{i\in I, j\in J, k\in L} T_{i,j} \cdot m_{i,j,k}^{emission} + \sum_{i\in WR, j\in J, k\in L} NR \cdot T_{i,j} \cdot m_{i,j,k}^{recycle} \right) \tag{34}$$

If we consider the revenue from selling glycerol, fertilizer, and biogas to be a credit of the biofuel production, the revenue, calculated by Eq. 35, offsets part of the annualized cost. We also assume the carbon dioxide in the raw biogas has been separated and recycled, so that biogas product possesses the same properties and price with natural gas. The total annualized cost is then defined by Eq. 36

$$credit = H \cdot \left\{ \frac{PRICE^{glycerol}}{\rho^{glycerol}} \cdot \sum_{j\in J} m_{8,j,34}^{down} + PRICE^{fer} \cdot \sum_{j\in J} \left( m_{8,j,27}^{down} + m_{9,j,27}^{down} \right) + \frac{PRICE^{ng}}{\rho^{ng}} \cdot \sum_{j\in J, k\in G} \left( m_{8,j,k}^{down} + m_{9,j,k}^{down} \right) \right\} \tag{35}$$

$$tac = aic + aoc - credit \tag{36}$$

As unit cost is one of the most significant factors to demonstrate the economic competitiveness of a biofuel product on a real market, one of the objective functions is defined by Eq. 37 as the ratio of the total annualized cost divided by the total GGE-based volume of the biofuel produced in a year

$$unit\_cost = \frac{tac}{gge} = \frac{a + \sum_{i\in I, j\in J} B_{i,j} \left( m_{i,j}^{cc} \right)^{SF_{i,j}}}{gge} \tag{37}$$

$$a = land\_cost \cdot \frac{IR \cdot (IR+1)^{LS}}{(IR+1)^{LS} - 1} + aoc - credit \tag{38}$$

$$B_{i,j} = P^K \cdot \frac{CC_{i,j}^b}{\left( MF_{i,j}^b \right)^{SF_{i,j}}} \cdot \frac{CEPCI_{i,j}}{CEPCI_{i,j}^b} \cdot \frac{IR \cdot (IR+1)^{LS}}{(IR+1)^{LS} - 1} \tag{39}$$

### *Life cycle environmental impact analysis constraints*

The environmental impact of the algae processing network is analyzed via the life cycle optimization framework.[4–6,51–53] This methodology integrates multiobjective optimization with LCA and economic evaluation into a systematic framework that optimizes the environmental and economic performances simultaneously. We consider a "gate-to-gate" analysis in this study, and the system boundary includes all the activities within the algal processing network as well as steam and electricity generation. The functional unit is identified as 1 GGE of the biofuel produced. Specifically, this LCA concerns the environment impact of direct GHG emissions from the cultivation, remnant treatment, and utility generation as well as indirect GHG emissions associated with purchased electricity and steam. The annual life cycle inventories of direct GHG emission of species $k$ $lci_k^{de}$, indirect GHG emission of electricity $lci^{ele}$, and steam $lci^{steam}$ are calculated by Eqs. 40–42

$$lci_k^{de} = \sum_{i\in I, j\in J} T_{i,j} \cdot m_{i,j,k}^{emission} + \sum_{i\in WR, j\in J} NR \cdot T_{i,j} \cdot m_{i,j,k}^{recycle}, \qquad \forall k \in K \tag{40}$$

$$lci^{ele} = H \cdot \left( \sum_{i\in I} pc_i - pp \right) \tag{41}$$

$$lci^{steam} = H \cdot \left( \sum_{i\in I} hc_i - hp \right) \tag{42}$$

The life cycle inventory is then translated into GWP, which estimates the amount of radiated heat trapped by GHG emissions based on carbon dioxide. The GWP calculation in our study is based on a time horizon of 100 years.[54] As in Eq. 43, the total GWP is determined as the sum of the GWPs of different entries. $\varphi_k$, $\varphi^{ele}$, and $\varphi^{steam}$ are damage factors of the corresponding entries specified by the publications of the Intergovernmental Panel on Climate Change.[55] Finally, to capture the environmental impact associated with 1 functional unit of the biofuel product, the other objective function of this model is defined by Eq. 44 as the ratio of the total GWP divided by the total GGE-based product volume in a year

$$gwp = \sum_{k\in K} \left( \varphi_k \cdot lci_k^{de} \right) + \varphi^{ele} \cdot lci^{ele} + \varphi^{steam} \cdot lci^{steam} \tag{43}$$

$$unit\_gwp = \frac{gwp}{gge} \tag{44}$$

## Solution Approaches

The $\varepsilon$-constraint method is considered to solve the multiobjective optimization problem in this study.[56] We first transform the environmental objective into an additional bounding constraint and generate an auxiliary MINLP problem (P2)

$$\text{(P2)} \quad \begin{aligned} \min \ & unit\_cost = \frac{a + \sum_{i\in I, j\in J} B_{i,j} \left( m_{i,j}^{cc} \right)^{SF_{i,j}}}{gge} \\ \text{s.t.} \ & \text{mass balance constraints (1)–(18)} \\ & \text{energy balance constraints (19)–(24)} \\ & \text{economic evaluation constraints (25)–(39)} \\ & \text{life cycle environmental impact analysis constraints (40)–(44)} \\ & gwp \le \varepsilon \cdot gge \end{aligned}$$

In this way, the multiobjective optimization problem is transferred into a series of single-objective optimization problems, but the presence of separable concave terms and a fractional term in the objective function makes solving such a large-scale nonconvex MINLP problem computationally intractable. In fact, problem (P2) belongs to a mixed-integer nonlinear fractional program (MINFP), which is a special class of MINLPs. To optimize the nonconvex MINFP problem (P2), we propose a global optimization strategy that integrates a parametric algorithm and a branch-and-refine algorithm.

### *Parametric algorithm based on Newton's method for the mixed-integer fractional objective*

The most significant nonlinear property in (P2) involves the fractional term in the objective function. Due to the combinatorial nature and nonconvexity of the fractional term, general-purpose solvers might not be able to provide optimal solutions. However, parametric approaches based on root-finding methods prove to be very efficient for several types of MINFPs.[57] Therefore, we apply a parametric algorithm to handle the fractional terms. First, a new objective function is developed as shown in Eq. 45

$$obj^{cost}(UC)=a+\sum_{i\in I,j\in J} B_{i,j}\left(m_{i,j}^{cc}\right)^{SF_{i,j}}-UC\cdot gge \tag{45}$$

By switching the objective function, we obtain a parametric problem (P3), where $UC$ is the important parameter that keeps updating when the algorithm proceeds. As a result of parameterization, $obj^{cost}(UC)$ is concave, monotonically decreasing, continuous, and has bounded subgradients. It follows from these properties that the equation $obj^{cost}(UC)=0$ has only one solution, which is also the global optimal solution of the original function.

$$\begin{aligned}
&\min\ obj^{cost}(UC)=a+\sum_{i\in I,j\in J} B_{i,j}\left(m_{i,j}^{cc}\right)^{SF_{i,j}}\cdot UC\cdot gge\\
&\text{s.t.}\ \ \text{mass balance constraints}\ (1)-(18)\\
&\qquad\text{energy balance constraints}\ (19)-(24)\\
&\qquad\text{economic evaluation analysis constraints}\ (25)-(39)\\
&\qquad\text{life cycle environmental impact}\\
&\qquad\quad\text{analysis constraints}\ (40)-(44)\\
&\qquad gwp\ \le \varepsilon\cdot gge\\
&\qquad\text{new objective function}\ (45)
\end{aligned}\tag{p3}$$

In principle, a variety of root-finding algorithms are able to solve the parametric objective function (P3) when set to zero. In this study, we consider an exact parametric algorithm based on Newton's method.[57–60] The procedure of this algorithm is:

Step 1. Choose $UC=0$ in the first iteration, and set the iteration counter as 1.

Step 2. Solve problem (P3) and obtain the optimal solution denoted as $m_{i,j}^{cc,\Delta}$ and $gge^{\Delta}$.

Step 3. If the optimal objective function value is sufficiently small, stop and output $UC$ as the optimal objective function value of (P2); otherwise, update $UC=\frac{a+\sum_{i,j}B_{i,j}\left(m_{i,j}^{cc,\Delta}\right)^{SF_{i,j}}}{gge^{\Delta}}$, increase the iteration counter by 1, and go to step 2.

Overall, the parametric algorithm transforms the original fractional term to a difference term. Despite still resulting in a nonconvex MINLP to solve in each iteration of the parametric algorithm, it has less nonlinearity compared to the original formulation and allows for further reduction of nonlinear terms by other methods.

### *Branch-and-refine algorithm based on successive piecewise linear approximations for separable concave terms*

So far, after parametric transformation, the remaining nonlinear terms in (P3) are the concave functions for capital cost estimation in Eq. 25. To improve the computational efficiency, we consider a piecewise linear approximation to each of these concave functions.[61–63] In this work, we consider piecewise linear functions following the multiple-choice formulation as shown in Eqs. 46–52,[64,65] where $P=\{p1,p2,p3,p4...\}$ denotes the set of partition points, $PP_{i,j,p}$ denotes the value of partition point $p$

$$cc_{i,j}=\sum_{p\in P}\left(E_{i,j,p}w_{i,j,p}+F_{i,j,p}y_{i,j,p}\right),\qquad \forall i\in I,j\in J \tag{46}$$

$$\sum_{p\in P} y_{i,j,p}=1,\qquad \forall i\in I,j\in J \tag{47}$$

$$\sum_{p\in P} w_{i,j,p}=m_{i,j}^{cc},\qquad \forall i\in I,j\in J \tag{48}$$

$$PP_{i,j,p-1}\cdot y_{i,j,p}\le w_{i,j,p}\le PP_{i,j,p}\cdot y_{i,j,p},\qquad \forall i\in I,j\in J,p\in P \tag{49}$$

$$y_{i,j,p}\in\{0,1\},\quad w_{i,j,p}\ge 0,\qquad \forall i\in I,j\in J,p\in P \tag{50}$$

$$E_{i,j,p}=\frac{\frac{CC_{i,j}^{b}}{\left(MF_{i,j}^{b}\right)^{SF_{i,j}}}\left(\frac{CEPCI_{i,j}}{CEPCI_{i,j}^{b}}\right)\left[\left(PP_{i,j,p}\right)^{SF_{i,j}}-\left(PP_{i,j,p-1}\right)^{SF_{i,j}}\right]}{PP_{i,j,p}-PP_{i,j,p-1}},\quad \forall i\in I,j\in J,p\in P \tag{51}$$

$$F_{i,j,p}=CC_{i,j}^{b}\left(\frac{PP_{i,j,p}}{MF_{i,j}^{b}}\right)^{SF_{i,j}}\left(\frac{CEPCI_{i,j}}{CEPCI_{i,j}^{b}}\right)-E_{i,j,p}\cdot PP_{i,j,p},\quad \forall i\in I,j\in J,p\in P \tag{52}$$

We replace the nonlinear constraint 25 with Eqs. 46–52 and switch the objective function to a relaxed one defined in Eq. 53, resulting in a relaxed mixed-integer linear programming (MILP) formulation (P4)

$$obj^{cost,relaxed}(UC)=tac-UC\cdot gge \tag{53}$$

Due to the concave nature of the power function, its piecewise linear function is located strictly under the original function regardless of the number of line segments, creating solid underestimation of the original function (see Figure 3). As (P4) has the same feasible region with that of (P3), the optimal solution of (P4) is also a feasible solution of (P3). Furthermore, the optimal objective function value of (P4) provides a valid lower bound to the global optimal solution, whereas the corresponding feasible objective solution of (P3) provides a valid upper bound. As the relaxed linear formulation can be solved efficiently by the branch-and-cut methods

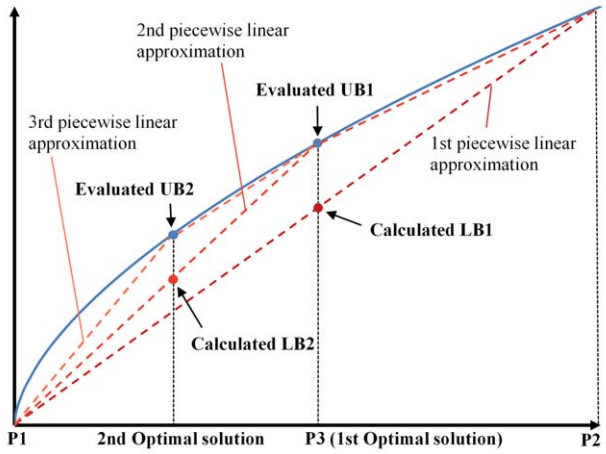


**Figure 3. An illustrative example being solved by the branch-and-refine algorithm.**

**[Color figure can be viewed in the online issue, which is available at wileyonlinelibrary.com.]**

implemented in solvers such as CPLEX, the remaining challenge is how to refine the solution and improve the accuracy of the approximation functions so that the global optimal solution can be obtained in finite iterations

$$
\begin{aligned}
&\min\ obj^{cost,relaxed}(UC) = tac - UC \cdot gge \\
&\text{s.t. mass balance constraints } (1)-(18) \\
&\qquad \text{energy balance constraints } (19)-(24) \\
&\qquad \text{economic evaluation constraints} \\
&\qquad (26)-(39),(46)-(52) \\
&\qquad \text{life cycle environmental impact analysis} \\
&\qquad \text{constraints } (40)-(44) \\
&\qquad gwp \le \varepsilon \cdot gge \\
&\qquad \text{relaxed new objective function } (53)
\end{aligned}
\tag{p4}
$$

Figure 3 demonstrates the first and the second iterations of an illustrative example of the branch-and-refine algorithm. In the first step, we set up an approximation with only one piece and solve the MILP problem to global optimality. If the lower bound is not close enough to the upper bound and this point is not too close to the existing partition points, we add this optimal solution as a new partition point and reconstruct the piecewise linear function with higher resolution. After the new linear formulation is well defined, we obtain and evaluate the lower and upper bounds in a similar manner. In this way, the branch-and-refine algorithm keeps iterating until lower and upper bounds are close enough to reach the optimality tolerance.

### *Global optimization strategy*

After the concave terms are approximated by piecewise linear functions in (P4), no more nonlinear terms remain. Implementing the branch-and-refine algorithm for (P4) returns the optimal solution of (P3), and this solution can be further examined by the parametric algorithm to see if the optimality criterion is satisfied or if another iteration is required. This procedure provides the fundamental idea of the global optimization strategy proposed in this study. The details of this strategy are shown in Figure 4.

We initialize the algorithm by setting $UC = 0$, the outer iteration counter $Iter^{out} = 1$, the lower bound $LB = 0$, the upper bound $UB = \infty$, and the inner iteration counter $Iter^{in} = 1$. We also provide a one-piece linear approximation for each concave function. As the branch-and-refine algorithm proceeds in the inner loop, the best upper bound decreases, while the best lower bound increases. As more partition points are added to approximate the concave power function, higher accuracy the piecewise linear approximation will be achieved. Once the optimal solution of (P3) is found in the inner loop, it is passed to the outer loop. If the optimal objective function value does not meet the stopping criterion, we update the parameters $UC$ and $Iter^{out}$ and restart the inner loop with the new objective function in Eq. 53. Otherwise, if the optimal objective function value is sufficiently small, the outer loop terminates and returns optimal solution $m*$ as well as the optimal unit annualized cost $UC$. The entire strategy relies only on an MILP solver and has the potential to significantly improve the computational performance when tackling large-scale superstructure optimization problems.

## Results and Discussions

All the computational experiments are performed on a Dell Optiplex 790 desktop with Intel(R) Core(TM) i5-2400 3.10GHz CPU, 8GB RAM and Windows 7 64-bit operating system. All the models and global optimization strategy are coded in GAMS 24.1.2.[66] Furthermore, the MILP problem (P4) is solved using CPLEX 12. The MINLP solvers utilized are BARON 12.3,[39] DICOPT, and SBB. The relative optimality tolerances of BARON 12.3,[39] DICOPT, and SBB are set to 0 and the absolute optimality tolerances for both of the parametric algorithm and the branch-and-refine algorithm and are set to $10^{-6}$.

### *Pareto-optimal curve*

We solve this MINLP problem by using the global optimization strategy in the previous section and obtain 20 optimal solutions, which constitute a Pareto-optimal curve as shown in Figure 5. The horizontal axis represents the unit GWP and the vertical axis represents unit annualized cost. The unit annualized cost decreases when unit GWP increases, which explicitly exhibits the trade-offs between the two objective functions. The Pareto-optimal curve separates the plane into a suboptimal region above the curve and an infeasible region beneath the curve. The economic or environmental (or both) performance of feasible points located in the suboptimal region can be improved by changing the processing route or operating conditions. However, the values of the optimal points cannot be improved simultaneously.

Judging from the shape of the curve, the optimal solutions are actually categorized into two groups corresponding to two optimal processing routes. The same processing route is identified between points A and B, and this processing route demonstrates lower unit environmental impact at the expense of higher unit annualized cost. As summarized in Table 1, the extreme point A of this group has the lowest unit GWP of 16.520 kg $CO_2$-eq/GGE but has the highest unit annualized cost of \$9.712/GGE. Conversely, the processing route selected by all the points between C and D favors lower unit

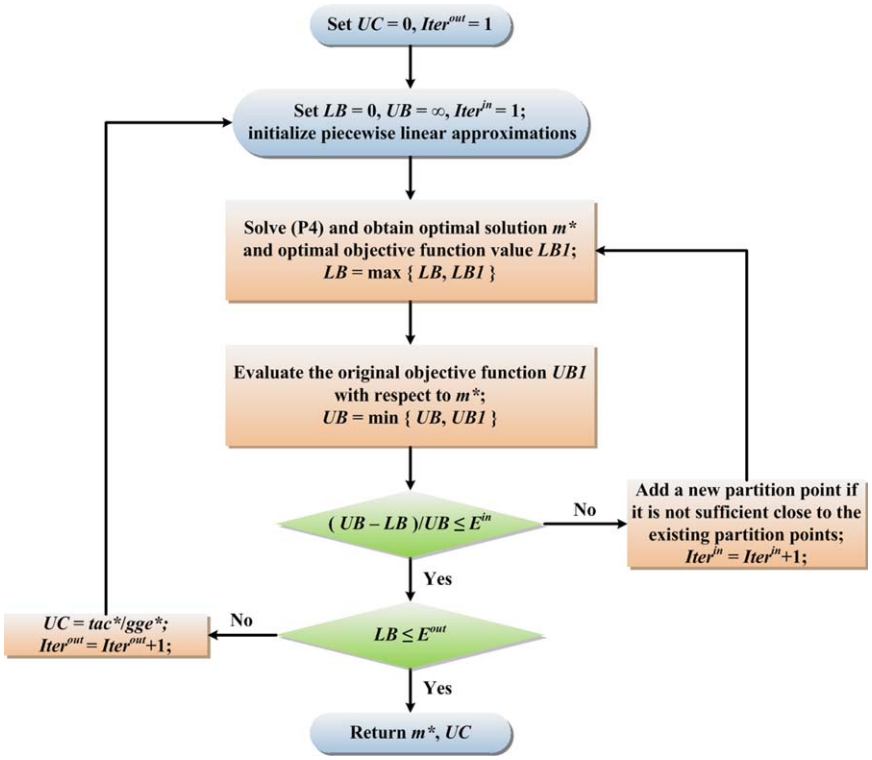


**Figure 4. Flowchart of the algorithm implemented.**

**[Color figure can be viewed in the online issue, which is available at wileyonlinelibrary.com.]**

annualized cost, but emits more GHG. The lowest unit annualized cost of \$7.017/GGE comes from point D which, unfortunately, incurs the highest unit GWP of 26.491 kg $CO_2$-eq/GGE.

As shown in Figure 6, the environmentally sustainable processing route of point A selects open pond cultivation, poly-$\gamma$-glutamic acid flocculation followed by a storage tank, HTL, HZSM-5-catalyzed Hyd., anaerobic digestion, electricity generation, and steam generation from the multiple technologies provided in the superstructure. The technology used for separating lipid materials from algae is HTL, which takes advantage of the wet microalgae biomass directly form harvesting section and breaks down the algal paste into lipid, remnant, biogas, and nutrient-rich water, thus avoiding the massive energy consumption for dewatering and lipid extraction. Nevertheless, the equipment dedicated to HTL is very costly, comprising more than 60% of the total equipment capital cost as shown in Figure 7a. As a result of choosing HTL, this processing route outperforms the others environmentally, but suffers economically.

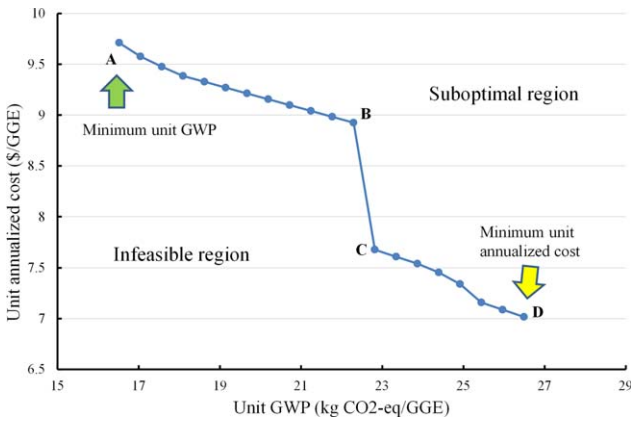


**Figure 5. Pareto-optimal curve for biofuel production.**

**[Color figure can be viewed in the online issue, which is available at wileyonlinelibrary.com.]**

Despite the same processing route between points A and B, other factors, such as the selection between the purchased electricity and the produced electricity from natural gas, also slightly contribute to the trade-offs between the conflicting objectives. The electricity from the grid is less expensive, but it causes large amount of indirect GHG emissions. However, if we purchase natural gas from the market and generate electricity onsite, half of the resulting off-gas is reused. Consequently, the direct GHG emissions of electricity generation are largely reduced, although extra capital cost to invest such a utility system is aggregated to the total cost. Similar trade-offs also exist between the purchased steam and the produced steam. Point A exhibits the lowest unit GWP on the Pareto-optimal curve, because it not only selects an environmentally sustainable processing route but also satisfies all the energy consumption by onsite utility generation.

As shown in Figure 8, the points between C and D choose open pond cultivation, poly-electrolyte flocculation, pressure

**Table 1. Primary Result Comparison Between Two Extreme Points**

| | Minimum Unit GWP (Point A) | Minimum Unit Annualized Cost (Point D) |
|---|---|---|
| Unit annualized cost (\$/GGE) | 9.712 | 7.017 |
| Unit GWP (kg $CO_2$-eq/GGE) | 16.520 | 26.491 |
| Energy product | Renewable diesel | Biodiesel |
| Throughput (million GGE) | 69.829 | 30.715 |

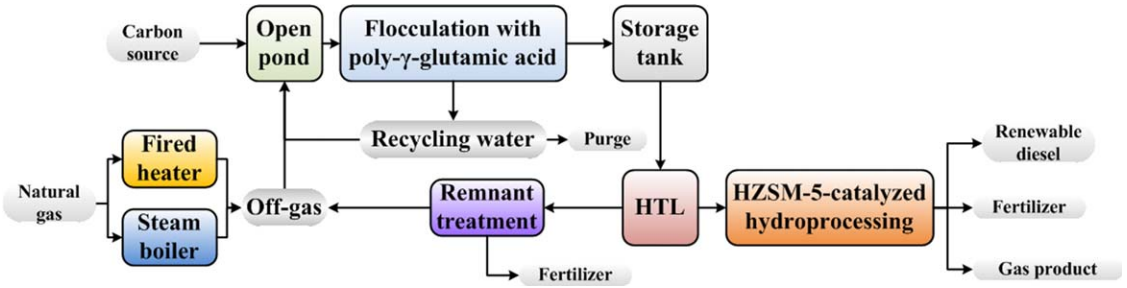


**Figure 6. Optimal processing route of point A.**

[Color figure can be viewed in the online issue, which is available at wileyonlinelibrary.com.]

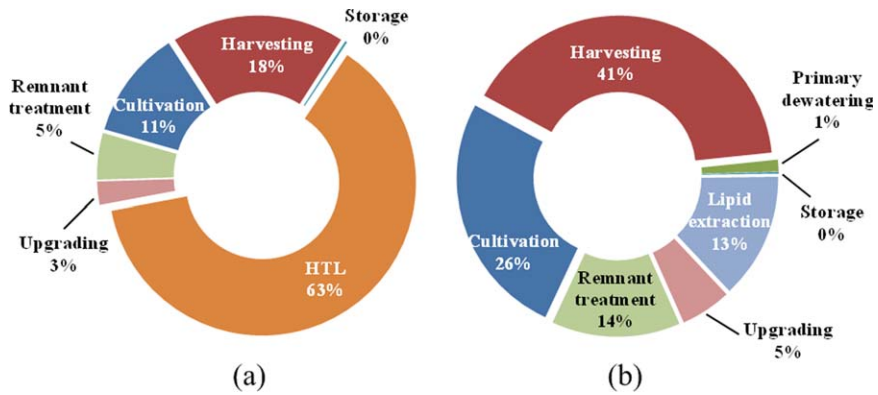


**Figure 7. Equipment capital cost distribution of (a) point A and (b) point D.**

[Color figure can be viewed in the online issue, which is available at wileyonlinelibrary.com.]

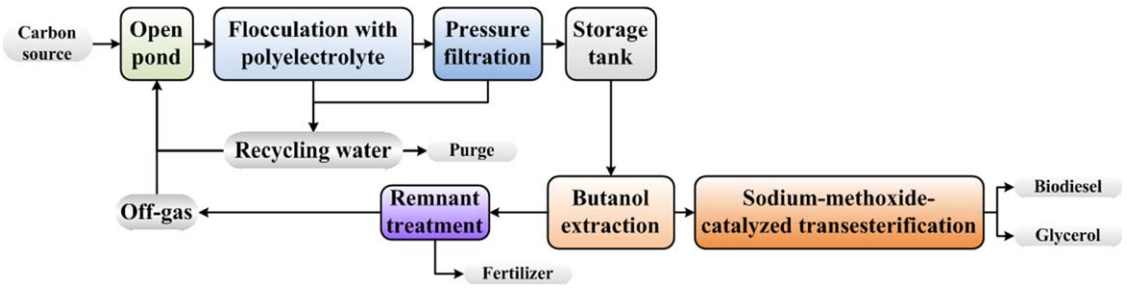


**Figure 8. Optimal processing route of point D.**

[Color figure can be viewed in the online issue, which is available at wileyonlinelibrary.com.]

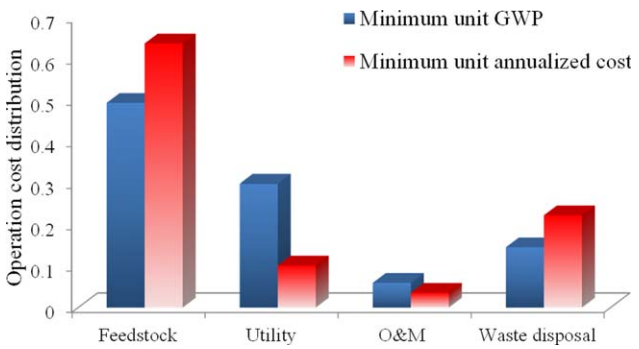


**Figure 9. Operation cost distributions of the minimum unit GWP processing route (point A) and minimum unit annualized cost processing route (point D).**

[Color figure can be viewed in the online issue, which is available at wileyonlinelibrary.com.]

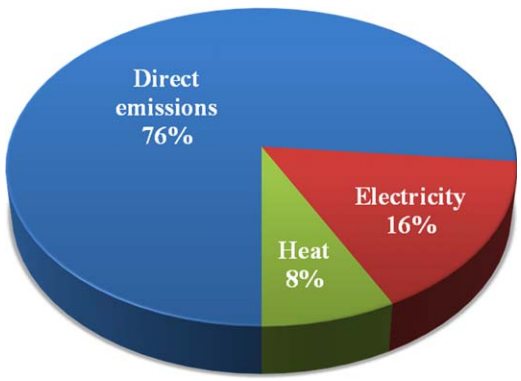


**Figure 10. Life cycle GWP distribution of the minimum unit annualized cost design (point D).**

[Color figure can be viewed in the online issue, which is available at wileyonlinelibrary.com.]

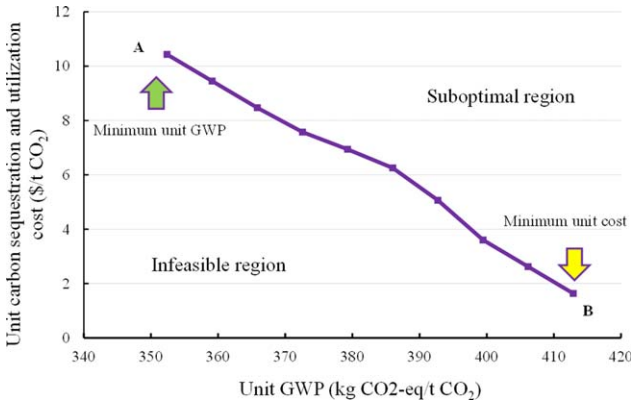


**Figure 11. Pareto-optimal curve for biological carbon sequestration.**

**[Color figure can be viewed in the online issue, which is available at wileyonlinelibrary.com.]**

filtration followed by a storage tank, butanol extraction for wet microalgae biomass, sodium-methoxide-catalyzed Trans., and anaerobic digestion. In contrast to the previous processing route, this route uses pressure filtration and butanol extraction. Furthermore, all the utility consumption of the extreme point D is satisfied by the external market, resulting in the lowest unit prices but highest unit environmental impact.

The breakdown of operation costs of the two extreme points is shown in Figure 9. Feedstock purchase cost takes the largest share in both processing routes, and more than 60% of the cost comes from makeup water, nitrogen, and phosphorus nutrients. The processing route with the lowest unit GWP (point A) purchases large amount of natural gas for utility generation, resulting in a very high utility cost. O&M costs rely on the annualized investment cost, so the higher equipment capital costs of point A render a larger share of O&M costs. The smaller contribution of waste disposal of point A is caused by the fact that HTL converts more bio-crude oil than physical extraction and leaves less waste materials to discharge.

Figure 10 illustrates the GWP distribution of point D. Direct GHG emissions dominate the GWP contribution as 25% of the incoming feed gas during the day bypasses the microalgae capture and is emitted to the atmosphere. The rest of the GWP comes from indirect GHG emissions of electricity (16%) and heat (8%) purchasing. Note that the processing route with the lowest unit GWP does not purchase utility, so the entirety of the GWP comes from emitting one quarter of the feed gas during the day and all the off-gas during the night.

### *Unit carbon sequestration and utilization cost for biological carbon sequestration*

Based on the optimal results in the last subsection, the unit annualized cost is in fact higher than the market prices of the fossil-derived counterparts. Alternatively, we further explore the economic and environmental behavior of the algae processing network as a system for biological carbon sequestration. For this purpose, we make two modifications in the model formulation (P1). First, we include the revenue of selling biofuel products into the term "*credit*" in Eq. 36; next, we replace the denominators in Eqs. 37 and 44 with the total amount of carbon dioxide sequestered in a year. As a result, the economic objective function is to minimize the unit carbon sequestration and utilization cost, whereas the environment objective function quantifies the unit GWP. Both objective functions are associated with the one ton of carbon dioxide sequestered by the algae processing network. The resulting multiobjective MINLP problem is solved using the proposed global optimization strategy and the optimization results are plotted in a Pareto-optimal curve shown in Figure 11.

In the new Pareto-optimal curve, when unit GWP increases, the unit carbon sequestration and utilization cost decreases. All 10 optimal points employ the same processing route. As illustrated in Figure 12, it includes open pond cultivation, poly-electrolyte flocculation, pressure filtration, a storage tank, butanol extraction, sodium-methoxide-catalyzed Trans., anaerobic digestion, and onsite energy generation. Despite selecting the same technologies, the 10 optimal points differ from each other with the ratio of energy generated on site divided by the total energy consumed. Two extreme points A and B are identified with the unit carbon sequestration and utilization costs of \$10.43/t of $CO_2$ and

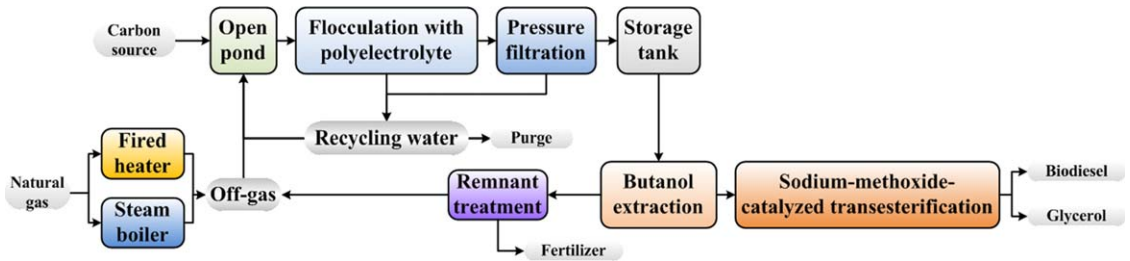


**Figure 12. Optimal processing route for biological carbon sequestration.**

**[Color figure can be viewed in the online issue, which is available at wileyonlinelibrary.com.]**

**Table 2. Problem Statistics of Point D**

| | | Relaxed MILP model (P4) | | |
|---|---|---|---|---|
| | Original MINLP Model (P1) | First Iteration | Second Iteration | Final Iteration |
| Number of discrete variables | 49 | 159 | 168 | 178 |
| Number of continuous variables | 32,958 | 33,068 | 33,077 | 33,087 |
| Number of constraints | 56,385 | 56,825 | 56,843 | 56,863 |

**Table 3. Computational Performance of Four Optimal Points**

| | Solving the MINLP model (P1) with BARON 12.3 directly | | Solving the MINLP model (P1) with DICOPT directly | | Solving the MINLP model (P1) with SBB directly | | Solving the MILP model (P4) with the proposed global optimization strategy | | |
|---|---|---|---|---|---|---|---|---|---|
| | Unit cost ($/GGE) | CPU limits(s) | Unit cost ($/GGE) | CPU(s) | Unit cost ($/GGE) | CPU(s) | Unit cost ($/GGE) | Iter. | CPU(s) |
| **A** | N/A[a] | 72,000 | Loc.Infeas.[c] | 84 | Loc.Infeas.[c] | 84 | 9.712 | 10 | 9 |
| **B** | N/A[b] | 72,000 | Loc.Infeas.[c] | 75 | Loc.Infeas.[c] | 74 | 8.925 | 6 | 3 |
| **C** | N/A[a] | 72,000 | Loc.Infeas.[c] | 76 | Loc.Infeas.[c] | 76 | 7.679 | 6 | 3 |
| **D** | N/A[a] | 72,000 | Loc.Infeas.[c] | 82 | Loc.Infeas.[c] | 77 | 7.017 | 6 | 3 |

[a]No upper and lower bound information is returned before the program reaches the computation time limit.
[b]The program automatically terminates due to solver failure after 4 h.
[c]"Loc.Infeas." represents "locally infeasible."

**Table 4. Lower and Upper Bounds in Solving the Optimization Problem of Point D**

| Outer iteration | Parameter *UC* | Inner iteration | Lower bound | Upper bound |
|---|---|---|---|---|
| 1 | 0 | 1 | 117.829 | 215.533 |
| | | 2 | 189.393 | 215.533 |
| | | 3 | 215.533 | 215.533 |
| 2 | 7.017 | 1 | −221.804 | 102.695 |
| | | 2 | −34.466 | 1.000 E −6 |
| | | 3 | 1.000 E −6 | 1.000 E −6 |

$1.64/t of $CO_2$, corresponding to unit GWP's of 352.41 kg $CO_2$-eq/t of $CO_2$ and 412.90 kg $CO_2$-eq/t of $CO_2$, respectively.

### *Computational performance*

The Pareto-optimal curve in Figure 5 is composed of 20 optimal points, consuming 114.04 CPUs in total. To demonstrate the performance of the proposed global optimization strategy, we consider point D for illustration. Problem sizes of the original MINLP model (P1) and the relaxed MILP model (P4) are summarized in Table 2. The relaxed MILP model (P4) evolves when the number of iteration increases, so we list the problem size of the first iteration, second iteration, and the final iteration.

To compare the performances of various optimization methods, we solve problem (P2) with the proposed global optimization strategy and several general-purpose MINLP solvers: BARON 12.3,[39] DICOPT, and SBB. The computational performances of these methods for four optimal points on the Pareto-optimal curve are listed in Table 3. Due to the combinatorial and nonconvex nature of (P2), the global optimizer BARON 12.3 fails to provide any valid results before the program reaches 20 h and is terminated. Local MINLP solvers DICOPT and SBB are very sensitive to the initial values and do not provide feasible results either. Although the number of iterations and computational time vary from point to point, no point exceeds 10 iterations and 10 CPUs when solving (P2) with the proposed global optimization strategy. Overall, for the large-scale superstructure optimization problem in this study, the proposed global optimization strategy demonstrates significant computational advantages over other general-purpose MINLP solvers.

The lower and upper bounds of each iteration of the optimization problem of point D with the proposed global optimization framework are shown in Table 4. The integrated algorithm takes two outer iterations to find the optimal objective function value of (P2) and for each outer iteration, the branch-and-refine algorithm takes three inner iterations to converge. During the inner loop, the best upper bound decreases as the number of the inner iteration increases, whereas the best lower bound keeps increasing until they are close enough to satisfy the inner stopping criterion. We notice that the gap between the best upper bound and lower bound reduces significantly in the second inner iteration, indicating the effective piecewise linear approximations of the original concave functions.

## Conclusions

In this work, we proposed a multiobjective MINLP model for the sustainable design and synthesis of an algae processing network involving 7800 processing routes. The MINLP model was formulated following a life cycle optimization framework to simultaneously optimize the unit annualized cost and unit GWP, both associated with the unit GGE of the final biofuel produced. To efficiently solve the nonconvex MINLP problem with separable concave terms and mixed-integer fractional terms in the objective functions, we proposed a global optimization strategy that integrated a branch-and-refine algorithm based on successive piecewise linear approximation and an exact parametric algorithm based on Newton's method. The proposed global optimization strategy significantly outperformed the other general-purpose MINLP solvers.

The bicriteria optimization problem was solved with the $\varepsilon$-constraint method, generating two Pareto-optimal curves for biofuel production and biological carbon sequestration, respectively. Three optimal processing routes are identified on the Pareto-optimal curves. From the biofuel production perspective, the most environmentally sustainable processing route achieved a unit GWP of 16.520 kg $CO_2$-eq/GGE and a unit annualized cost of $9.712/GGE, whereas the most economical processing route resulted in a unit annualized cost of $7.017/GGE and a unit GWP of 26.791 kg $CO_2$-eq/GGE. If the algae processing network is used for biological carbon sequestration, the unit carbon sequestration and utilization cost ranges from $10.43/t of $CO_2$ to $1.64/t of $CO_2$, corresponding to unit GWP's from 352.41 kg $CO_2$-eq/t of $CO_2$ to 412.90 kg $CO_2$-eq/t of $CO_2$, respectively.

The proposed global optimization strategy is very efficient in solving the problem in this work. However, for a larger problem, the resulting MILP problem could be computationally intractable if too many partition points are added. An improved approach, which imposes constraints to limit the total partition points, will be developed in the future work.

## Acknowledgment

The financial support from the Initiative for Sustainability and Energy at Northwestern (ISEN) is gratefully acknowledged.

## Notation

### Sets/indices

$I$ = set of sections indexed by $i$
$J$ = set of technological alternatives indexed by $j$
$K$ = set of species indexed by $k$. The 37 species represent, respectively $H_2O$, $CO_2$, $N_2$, $O_2$, $H_2$, CO, $CH_4$, $C_2H_6$, $C_3H_8$, $C_4H_{10}$, $C_5H_{12}$, polyelectrolyte, sodium hydroxide (flocculant), poly-aluminum chloride, aluminum sulfate, chitosan, poly-$\gamma$-glutamic acid, N, P, algae, salt, lipid, remnant, hexane, isopropanol/hexane, butanol, solid, $CH_4O$, NaOH (catalyst), $H_2SO_4$, lipase, $CH_3NaO$, heterogeneous catalyst, glycerol, soap, biodiesel, and renewable diesel.
$N$ = set of name of flows $n$
$P$ = set of partition point indexed by $p$

### Subsets

$C_i$ = subset of species that contribute to $m_{i,j}^{cc}$ in section $i$
$D_i$ = subset of sections whose "down" flows go to section $i$
$G$ = subset of species that are the major components in natural gas
$L$ = subset of liquid species
$R_i$ = subset of sections whose "recycle" flows go to section $i$
$WR$ = subset of sections whose "recycle" flow is discharged during the nights

### Parameters

$B_{i,j}$ = parameter in the definition of unit cost
$CC_{i,j}^{b}$ = capital cost of technology $j$ in section $i$ in the base case
$CEPCI_{i,j}$ = chemical engineering plant cost index of technology $j$ in section $i$ in the current year
$CEPCI_{i,j}^{b}$ = chemical engineering plant cost index of technology $j$ in section $i$ in the reference year
$E_{i,j,p}$ = parameter of point $p$ used in piecewise linear approximation
$E^{in}$ = optimality margin of the inner loop
$E^{out}$ = optimality margin of the outer loop
$F_{i,j,p}$ = parameter of point $p$ used in piecewise linear approximation
$GGE_k$ = GGE conversion coefficient of species $k$
$gge*$ = the optimal solution of variable gge in the inner loop
$H$ = annual working hours
$IR$ = interest rate
$Iter^{in}$ = iteration counter of the inner loop
$Iter^{out}$ = iteration counter of the outer loop
$LB$ = current lower bound
$LB1$ = the optimal objective function value of one iteration in the inner loop
$LHV_k$ = lower heating value of species $k$
$LS$ = life span of the algal process
$m*$ = the optimal solution of one iteration in the inner loop
$M^{fg}$ = total mass flow rate of the flue gas
$MF_{i,j}^{b}$ = mass flow rate of technology $j$ in section $i$ in the base case
$NR$ = ratio of night hours divided by the total hours in a day
$P_{i,j,k,k'}^{in}$ = inlet concentration of species $k$ based on species $k'$ of technology $j$ in section $i$
$P^{K}$ = multiplier of the project investment cost based on the capital cost
$P^{om}$ = multiplier of the O&M cost based on the annualized investment cost
$PP_{i,j,p}$ = partition point value of point $p$ used in piecewise linear approximation
$PRICE_k$ = price of species $k$
$PRO_j^a$ = area productivity of technology $j$ in the cultivation section
$SC_{i,j,k,k'}$ = stoichiometric coefficient of species $k$ based on species $k'$ of technology $j$ in section $i$
$SF_{i,j}$ = sizing factor of technology $j$ in section $i$
$SF_{i,j,k,k'}^{down}$ = split fraction of species $k$ to the down flow based on species $k'$ of technology $j$ in section $i$
$SF_{i,j,k}^{emission}$ = split fraction of species $k$ to the emission flow of technology $j$ in section $i$
$T_{i,j}$ = operating time of technology $j$ in section $i$
$tac*$ = the optimal solution of variable tac in the inner loop
$UB$ = current upper bound
$UB^{m}$ = sufficiently large number in logic constraints
$UB1$ = feasible objective function value evaluated by the optimal solution $m*$
$UC$ = auxiliary parameter in economic objective in the transformed formulation
$UHC_{i,j,k}$ = unit heat consumption of species $k$ technology $j$ in section $i$
$UPC_{i,j,k}$ = unit power consumption of species $k$ technology $j$ in section $i$
$WF_k^{fg}$ = weight fraction of species $k$ in the flue gas
$WF_k^{ng}$ = weight fraction of species $k$ in the natural gas
$X_{i,j}$ = reaction conversion of technology $j$ in section $i$
$Y^{com}$ = efficiency of combustion
$Y^{he}$ = energy efficient of heat exchanger
$Y^{turbine}$ = energy efficient of turbine
$\varepsilon$ = parameter for $\varepsilon$-constraint method
$\rho^k$ = density of species $k$
$\varphi_k$ = damage factor of species $k$
$\varphi^{ele}$ = damage factor of electricity
$\varphi^{steam}$ = damage factor of steam

### Binary variables

$y_{i,j}$ = 0–1 variable. Equal to 1 if the technology $j$ in section $i$ is the selected
$y_{i,j,p}$ = 0–1 variable. Equal to 1 if the point $p$ in technology $j$ in section $i$ is the selected

### Nonnegative continuous variables

$a$ = parameter in the definition of unit cost
$aic$ = annualized investment cost
$aoc$ = annual operation cost
$cc_{i,j}$ = capital cost of technology $j$ in section $i$
$credit$ = income from selling byproducts
$fsc$ = feedstock cost
$gge$ = annual biofuel volume produced on a GGE basis, million GGE
$gwp$ = GWP
$hc_i$ = heat consumption of section in section $i$
$hp$ = total heat production
$land\_cost$ = land cost
$lci_k^{de}$ = life cycle inventory of species $k$ counted as direct emissions
$lci^{ele}$ = life cycle inventory of electricity
$lci^{steam}$ = life cycle inventory of steam
$m_{i,j}^{cc}$ = mass flow rate for capital cost evaluation of technology $j$ in section $i$, t/h
$m_{i,j,k}^{n}$ = mass flow rate of species $k$ in flow $n$ of technology $j$ in section $i$, t/h
$m^{ng1}$ = total mass flow rate of the natural gas to generate electricity, t/h
$m^{ng2}$ = total mass flow rate of the natural gas to generate heat, t/h
$obj^{cost}(UC)$ = economic objective function of the transformed formulation
$obj^{cost,relaxed}(UC)$ = relaxed economic objective function of the transformed formulation
$omc$ = O&M cost
$pc_i$ = power consumption of section in section $i$
$pp$ = total power production
$tac$ = total annualized cost
$tpic$ = total project investment cost
$unit\_cost$ = unit annualized cost
$unit\_gwp$ = unit GWP
$utility$ = utility cost
$w_{i,j,p}$ = auxiliary variable of point $p$
$waste$ = waste disposal cost

## Literature Cited


1. Daoutidis P, Marvin WA, Rangarajan S, Torres AI. Engineering biomass conversion processes: a systems perspective. *AIChE J*. 2013; 59(1):3–18.
2. Ferrell J, Sarisky-Reed V. National algal biofuels technology roadmap. College Park, MD: US Department of Energy, 2010.
3. Yue D, You F, Snyder SW. Biomass-to-bioenergy and biofuel supply chain optimization: overview, key issues and challenges. *Comput Chem Eng*. 2014;66:36–56.
4. Yue DJ, Kim MA, You FQ. Design of sustainable product systems and supply chains with life cycle optimization based on functional unit: general modeling framework, mixed-integer nonlinear

programming algorithms and case study on hydrocarbon biofuels. *ACS Sustain Chem Eng*. 2013;1(8):1003–1014.
5. Wang B, Gebreslassie BH, You FQ. Sustainable design and synthesis of hydrocarbon biorefinery via gasification pathway: integrated life cycle assessment and technoeconomic analysis with multiobjective superstructure optimization. *Comput Chem Eng. 10* 2013;52:55–76.
6. Gebreslassie BH, Waymire R, You F. Sustainable design and synthesis of algae-based biorefinery for simultaneous hydrocarbon biofuel production and carbon sequestration. *AIChE J*. 2013;59(5):1599–1621.
7. Chisti Y. Biodiesel from microalgae. *Biotechnol Adv*. 2007;25(3): 294–306.
8. Brennan L, Owende P. Biofuels from microalgae-A review of technologies for production, processing, and extractions of biofuels and co-products. *Renew Sustain Energy Rev*. 2010;14(2):557–577.
9. Kim J, Yoo G, Lee H, Lim J, Kim K, Kim CW, Park MS, Yang JW. Methods of downstream processing for the production of biodiesel from microalgae. *Biotechnol Adv*. 2013;31(6):862–876.
10. Lee AK, Lewis DM, Ashman PJ. Disruption of microalgal cells for the extraction of lipids for biofuels: processes and specific energy requirements. *Biomass Bioenerg*. 2012;46:89–101.
11. Halim R, Danquah MK, Webley PA. Extraction of oil from microalgae for biodiesel production: a review. *Biotechnol Adv*. 2012;30(3): 709–732.
12. Barreiro DL, Prins W, Ronsse F, Brilman W. Hydrothermal liquefaction (HTL) of microalgae for biofuel production: state of the art review and future prospects. *Biomass Bioenerg*. 2013;53:113–127.
13. Uduman N, Qi Y, Danquah MK, Forde GM, Hoadley A. Dewatering of microalgal cultures: a major bottleneck to algae-based fuels. *J Renew Sustain Energy* 2010;2(1):012701.
14. Alabi AO, Bibeau E, Tampier M, Council BCI. Microalgae Technologies & Processes for Biofuels-bioenergy Production in British Columbia: Current Technology, Suitability & Barriers to Implementation: Final Report. British Columbia Innovation Council, Vancouver, BC, Canada, 2009.
15. Davis R, Aden A, Pienkos PT. Techno-economic analysis of autotrophic microalgae for fuel production. *Appl Energy* 2011;88(10):3524–3531.
16. Davis R, Aden A. Renewable Diesel from Algal Lipids: an Integrated Baseline for Cost, Emissions, and Resource Potential from a Harmonized Model. Argonne National Laboratory, Lemont, IL, USA, 2012.
17. Delrue F, Seiter PA, Sahut C, Cournac L, Roubaud A, Peltier G, Froment AK. An economic, sustainability, and energetic model of biodiesel production from microalgae. *Bioresour Technol*. 2012;111: 191–200.
18. Delrue F, Li-Beisson Y, Setier PA, Sahut C, Roubaud A, Froment AK, Peltier G. Comparison of various microalgae liquid biofuel production pathways based on energetic, economic and environmental criteria. *Bioresour Technol*. 2013;136:205–212.
19. Pokoo-Aikins G, Nadim A, El-Halwagi MM, Mahalec V. Design and analysis of biodiesel production from algae grown through carbon sequestration. *Clean Technol Environ*. 2010;12(3):239–254.
20. Sanchez E, Ojeda K, El-Halwagi M, Kafarov V. Biodiesel from microalgae oil production in two sequential esterification/transesterification reactors: pinch analysis of heat integration. *Chem Eng J*. 2011;176:211–216.
21. Silva C, Soliman E, Cameron G, Fabiano LA, Seider WD, Dunlop EH, Coaldrake AK. Commercial-scale biodiesel production from algae. *Ind Eng Chem Res*. 2014;53(13):5311–5324.
22. Lardon L, Helias A, Sialve B, Steyer JP, Bernard O. Life-Cycle Assessment of Biodiesel Production from Microalgae. *Environ Sci Technol*. 2009;43(17):6475–6481.
23. Brentner LB, Eckelman MJ, Zimmerman JB. Combinatorial Life Cycle Assessment to inform process design of industrial production of algal biodiesel. *Environ Sci Technol*. 2011;45(16):7060–7067.
24. Frank E, Han J, Palou-Rivera I, Elgowainy A, Wang M. Life-cycle analysis of algal lipid fuels with the greet model. Center for Transportation Research, Energy Systems Division, Argonne National Laboratory, Oak Ridge, 2011.
25. Frank ED, Elgowainy A, Han J, Wang ZC. Life cycle comparison of hydrothermal liquefaction and lipid extraction pathways to renewable diesel from algae. *Mitig Adapt Strat Global Change* 2013;18(1):137–158.
26. Collet P, Helias A, Lardon L, Ras M, Goy RA, Steyer JP. Life-cycle assessment of microalgae culture coupled to biogas production. *Bioresour Technol*. 2011;102(1):207–214.
27. Martin M, Grossmann IE. Optimal engineered algae composition for the integrated simultaneous production of bioethanol and biodiesel. *AIChE J*. 2013;59(8):2872–2883.
28. Baliban RC, Elia JA, Floudas CA, Xiao X, Zhang ZJ, Li J, Cao HB, Ma J, Qiao Y, Hu XT. Thermochemical conversion of duckweed biomass to gasoline, diesel, and jet fuel: process synthesis and global optimization. *Ind Eng Chem Res*. 2013;52(33):11436–11450.
29. Chen Y, Adams TA, Barton PI. Optimal design and operation of flexible energy polygeneration systems. *Ind Eng Chem Res*. 2011; 50(8):4553–4566.
30. Chen Y, Li X, Adams TA, Barton PI. Decomposition strategy for the global optimization of flexible energy polygeneration systems. *AIChE J*. 2012;58(10):3080–3095.
31. Liu P, Pistikopoulos EN, Li Z. A Multi-objective optimization approach to polygeneration energy systems design. *AIChE J*. 2010; 56(5):1218–1234.
32. El-Halwagi AM, Rosas C, Ponce-Ortega JM, Jimenez-Gutierrez A, Mannan MS, El-Halwagi MM. Multiobjective optimization of biorefineries with economic and safety objectives. *AIChE J*. 2013;59(7): 2427–2434.
33. Hipolito-Valencia BJ, Rubio-Castro E, Ponce-Ortega JM, Serna-Gonzalez M, Napoles-Rivera F, El-Halwagi MM. Optimal design of inter-plant waste energy integration. *Appl Therm Eng*. 2014;62(2): 633–652.
34. Rizwan M, Lee JH, Gani R. Optimal processing pathway for the production of biodiesel from microalgal biomass: a superstructure based approach. *Comput Chem Eng*. 2013;58:305–314.
35. Cheali P, Gernaey KV, Sin G. Toward a computer-aided synthesis and design of biorefinery networks: data collection and management using a generic modeling approach. *ACS Sustain Chem Eng*. 2014; 2(1):19–29.
36. Zondervan E, Nawaz M, de Haan AB, Woodley JM, Gani R. Optimal design of a multi-product biorefinery system. *Comput Chem Eng*. 2011;35(9):1752–1766.
37. Quaglia A, Sarup B, Sin G, Gani R. Integrated business and engineering framework for synthesis and design of enterprise-wide processing networks. *Comput Chem Eng*. 2012;38:213–223.
38. Gong J, You F. Optimal design and synthesis of algal biorefinery processes for biological carbon sequestration and utilization with zero direct greenhouse gas emissions: MINLP model and global optimization algorithm. *Ind Eng Chem Res*. 2014;53(4):1563–1579.
39. Tawarmalani M, Sahinidis NV. A polyhedral branch-and-cut approach to global optimization. *Math Program*. 2005;103(2):225–249.
40. Andrews K. Technology to reduce flue gas emissions from existing power plants. 2012; www.myninesigma.com/_layouts/RFPs/NineSigma_RFP_67698.pdf. Accessed on January 3, 2014.
41. Gouveia L. Microalgae as a Feedstock for Biofuels. Springer, New York, NY, USA, 2011.
42. Grima EM, Belarbi EH, Fernandez FGA, Medina AR, Chisti Y. Recovery of microalgal biomass and metabolites: process options and economics. *Biotechnol Adv*. 2003;20(7–8):491–515.
43. Lee JY, Yoo C, Jun SY, Ahn CY, Oh HM. Comparison of several methods for effective lipid extraction from microalgae. *Bioresour Technol*. 2010;101:S75–S77.
44. Valdez PJ, Nelson MC, Wang HY, Lin XXNN, Savage PE. Hydrothermal liquefaction of *Nannochloropsis* sp.: systematic study of process variables and analysis of the product fractions. *Biomass Bioenerg*. 2012;46:317–331.
45. Halim R, Gladman B, Danquah MK, Webley PA. Oil extraction from microalgae for biodiesel production. *Bioresour Technol*. 2011; 102(1):178–185.
46. Bollmeier W, Sprague S, No F. Aquatic Species Program. Solar Energy Research Inst.: Golden, CO, 1989.
47. Li Z, Savage PE. Feedstocks for fuels and chemicals from algae: treatment of crude bio-oil over HZSM-5. *Algal Res*. 2013;2(2):154–163.
48. Woods MC, Capicotto P, Haslbeck JL, Kuehn NJ, Matuszewski M, Pinkerton LL, Rutkowski MD, Schoff RL, Vaysman V. Cost and performance baseline for fossil energy plants. Vol. 1, Bituminous Coal and Natural Gas to Electricity Final Report. National Energy Technology Laboratory, Morgantown, WV, USA, 2007.
49. US Department of Energy LBNL, Resource Dynamic Corporation. Improving Steam System Performance: A Sourcebook for Industry, US Department of Energy LBNL, Washington, D.C., USA, 2004.
50. Seider WD, Seader JD, Lewin DR. Product & Process Design Principles: Synthesis, Analysis and Evaluation. Wiley, Hoboken, NJ, USA, 2009.

51. You FQ, Wang B. Life cycle optimization of biomass-to-liquid supply chains with distributed-centralized processing networks. *Ind Eng Chem Res*. 2011;50(17):10102–10127.
52. Gebreslassie BH, Slivinsky M, Wang BL, You FQ. Life cycle optimization for sustainable design and operations of hydrocarbon biorefinery via fast pyrolysis, hydrotreating and hydrocracking. *Comput Chem Eng*. *5* 2013;50:71–91.
53. Zhang Q, Gong J, Skwarczek M, Yue D, You F. Sustainable process design and synthesis of hydrocarbon biorefinery through fast pyrolysis and hydroprocessing. *AIChE J*. 2014;60(3):980–994.
54. Plattner G-K, Stocker T, Midgley P, Tignor M. IPCC Expert Meeting on the Science of Alternative Metrics, Meeting Report. Oslo, Norway, 2009.
55. Metz B, Davidson O, de Coninck H, Loos M, Meyer L. IPCC Special Report on Carbon Dioxide Capture and Storage: Intergovernmental Panel on Climate Change, Geneva (Switzerland). Working Group III, New York, NY, USA, 2005.
56. Hwang CL, Masud ASM. Multiple Objective Decision Making-Methods and Applications. Vol. 164. Springer, New York, NY, USA, 1979.
57. Zhong ZX, You FQ. Globally convergent exact and inexact parametric algorithms for solving large-scale mixed-integer fractional programs and applications in process systems engineering. *Comput Chem Eng*. 2014;61:90–101.
58. Yue DJ, You FQ. Sustainable scheduling of batch processes under economic and environmental criteria with MINLP models and algorithms. *Comput Chem Eng*. 2013;54:44–59.
59. Chu YF, You FQ. Integration of scheduling and control with online closed-loop implementation: fast computational strategy and large-scale global optimization algorithm. *Comput Chem Eng*. 2012;47:248–268.
60. Chu YF, You FQ. Integration of production scheduling and dynamic optimization for multi-product CSTRs: generalized Benders decomposition coupled with global mixed-integer fractional programming. *Comput Chem Eng*. 2013;58:315–333.
61. Yue DJ, You FQ. Planning and scheduling of flexible process networks under uncertainty with stochastic inventory: MINLP models and algorithm. *AIChE J*. 2013;59(5):1511–1532.
62. You FQ, Pinto JM, Grossmann IE, Megan L. Optimal distribution-inventory planning of industrial gases. II. MINLP models and algorithms for stochastic cases. *Ind Eng Chem Res*. 2011;50(5):2928–2945.
63. You FQ, Grossmann IE. Stochastic inventory management for tactical process planning under uncertainties: MINLP models and algorithms. *AIChE J*. 2011;57(5):1250–1277.
64. Croxton KL, Gendron B, Magnanti TL. A comparison of mixed-integer programming models for nonconvex piecewise linear cost minimization problems. *Manage Sci*. 2003;49(9):1268–1273.
65. Padberg M. Approximating separable nonlinear functions via mixed zero-one programs. *Oper Res Lett*. 2000;27(1):1–5.
66. Rosenthal RE. GAMS—A User's Guide. GAMS Development Corporation, Washington, DC, USA, 2014.

*Manuscript received Mar. 25, 2014, and revision received May 7, 2014.*